

Photoproduction of hidden-charm states in the $\gamma p \rightarrow \bar{D}^{*0} \Lambda_c^+$ reaction near threshold ^{*}

Yin Huang (黄银)^{1,2,3;1)} Ju-Jun Xie (谢聚军)^{1,3;2)} Jun He (何军)^{1,3} Xurong Chen (陈旭荣)^{1,3}
Hong-Fei Zhang (张鸿飞)^{2,3}

¹ Research Center for Hadron and CSR Physics, Lanzhou University and Institute of Modern Physics of CAS, Lanzhou 730000, China

² School of Nuclear Science and Technology, Lanzhou University, Lanzhou 730000, China

³ Institute of Modern physics, Chinese Academy of Sciences, Lanzhou 730000, China

Abstract:

We report on a theoretical study of the hidden charm $N_{c\bar{c}}^*$ states in the $\gamma p \rightarrow \bar{D}^{*0} \Lambda_c^+$ reaction near threshold within an effective Lagrangian approach. In addition to the contributions from the s -channel nucleon pole, the t -channel D^0 exchange, the u -channel Λ_c^+ exchange and the contact term, we study the contributions from the $N_{c\bar{c}}^*$ states with spin-parity $J^P = 1/2^-$ and $3/2^-$. The total and differential cross sections of the $\gamma p \rightarrow \bar{D}^{*0} \Lambda_c^+$ reaction are predicted. It is found that the contributions of these $N_{c\bar{c}}^*$ states give clear peak structures in the total cross sections. Thus, this reaction is another new platform to study the hidden-charm states. It is expected that our model calculation may be tested by future experiments.

Key words: Hidden charm states; Photon production; Effective Lagrangian approach

PACS: 14.40.Rt, 13.75.Gx, 25.80.Hp, 12.40.Vv

1 Introduction

The study of hadron states beyond the traditional quark model, namely the exotic states, has been a hot topic in hadron physics, and these studies will improve our understanding of non-perturbative QCD. With the experimental progress on this issue over the past decade, more and more evidence in the heavy quark sector indicates possible candidates for exotic states, which are called the XYZ states. However, experimental evidence for exotic pentaquark baryon states has been missing for a long time. Recently, the LHCb Collaboration reported two hidden-charm pentaquark states $P_c^+(4380)$ and $P_c^+(4450)$ in the $J/\psi p$ invariant mass spectrum from the $\Lambda_b^0 \rightarrow J/\psi p K^-$ decay [1], and their masses and widths are $M_{P_c(4380)} = 4380 \pm 8 \pm 29$ MeV, $\Gamma_{P_c(4380)} = 205 \pm 18 \pm 86$ MeV, $M_{P_c(4450)} = 4449.8 \pm 1.7 \pm 2.5$ MeV, $\Gamma_{P_c(4450)} = 39 \pm 5 \pm 19$ MeV. Since the two states were reported from the final state $J/\psi p$ invariant mass distribution, the isospin of the $P_c(4380)$ and $P_c(4450)$ is $1/2$ and they are ideal candidates for pentaquark states with quark

content of $c\bar{c}uud$. According to partial wave analysis, the preferred spin-parity J^P of the $P_c(4380)$ and the $P_c(4450)$ are either $\frac{3}{2}^-$ and $\frac{5}{2}^+$ or $\frac{3}{2}^+$ and $\frac{5}{2}^-$, respectively. After this, various explanations for the $P_c(4380)$ and $P_c(4450)$ states were proposed from the theoretical side (see more details in a recent review paper [2]). However, the structure of these two states is still an open question, and none of the explanations in the literature have been accepted unanimously.

Actually, predictions of hidden charm baryon states have been made before. In Ref. [3], loosely bound hidden charm molecular baryons composed of anti-charmed meson and charmed baryon were obtained with the one-boson-exchange model. In Refs. [4, 5], the interaction between various anti-charmed mesons and charmed baryons plus decay channels in the light sector was studied within the framework of the coupled-channel unitary approach. Several dynamically generated $N_{c\bar{c}}^*$ and $\Lambda_{c\bar{c}}^*$ resonances with hidden charm were predicted with mass above 4 GeV and width smaller than 100 MeV [4, 5]. Us-

Received 20 June 2016

^{*} Supported by the Major State Basic Research Development Program in China (No. 2014CB845400), the National Natural Science Foundation of China (Grants No. 11475227, No. 11275235, No. 11035006) and the Chinese Academy of Sciences (the Knowledge Innovation Project under Grant No. KJCX2-EW-N01). It is also supported by the Youth Innovation Promotion Association CAS (No. 2016367) and by the Open Project Program of State Key Laboratory of Theoretical Physics, Institute of Theoretical Physics, Chinese Academy of Sciences, China (No. Y5KF151CJ1)

1) E-mail: huangy2014@lzu.cn

2) E-mail: xiejujun@impcas.ac.cn

©2013 Chinese Physical Society and the Institute of High Energy Physics of the Chinese Academy of Sciences and the Institute of Modern Physics of the Chinese Academy of Sciences and IOP Publishing Ltd

ing Heavy Quark Spin Symmetry and the local hidden gauge approach, further studies were done in Ref. [6] and similar results to those of Refs. [4, 5] were found in the study of the interaction of the $J/\psi N$, $\bar{D}^* \Lambda_c$, $\bar{D}^* \Sigma_c$, $\bar{D} \Sigma_c^*$, and $\bar{D}^* \Sigma_c^*$ coupled channels. In the $I = 1/2$ sector, three states with $J^P = 1/2^-$ and three states with $J^P = 3/2^-$ were dynamically generated [6] (see table I of that paper). Based on the results of Refs. [4–6], the molecule nature, $\bar{D}^* \Sigma_c - \bar{D}^* \Sigma_c^*$ molecular states, of the above two P_c states was proposed in Refs. [7, 8]. Besides, the nature of the $P_c(4380)$ was investigated in Ref. [9], and it was found that the decays of the $P_c(4380)$ to $\bar{D}^* \Lambda_c$ and $J/\psi p$ are very different for $P_c(4380)$ being the $\bar{D} \Sigma_c^*$ and the $\bar{D}^* \Sigma_c$ molecule states. Hence, the study of the $P_c(4380)$ states in the $\bar{D}^* \Lambda_c$ is important to disentangle the nature of the $P_c(4380)$ states.

There have also been phenomenology studies on the production of those hidden charm states from scattering processes. In Refs. [10–12], the role of the P_c states were studied in the $\gamma p \rightarrow P_c^+ \rightarrow J/\psi p$ reaction, while in Refs. [13–15], the role played by the hidden charm states were discussed in the π beam induced reactions of $\pi^- p \rightarrow \eta_c n$, $\pi^- p \rightarrow J/\psi n$, and $\pi^- p \rightarrow D^- \Sigma_c^+$. Along this line, in this work, we study the role of these hidden charm N_{cc}^* states in the $\gamma p \rightarrow \bar{D}^{*0} \Lambda_c^+$ reaction near the reaction threshold within the effective Lagrangian approach. Unfortunately, the couplings of the two observed $P_c(4380)$ and $P_c(4450)$ states to the γN and $\bar{D}^* \Lambda_c$ channels are unknown, so we will take the work of Ref. [6] as a reference where the couplings of these N_{cc}^* to $J/\psi p$ and $\bar{D}^* \Lambda_c$ were obtained. We then provide the total and differential cross sections of the $\gamma p \rightarrow \bar{D}^{*0} \Lambda_c^+$ reaction. It is found that the differential cross sections for the N_{cc}^* states with different quantum numbers are different, which can be used to

distinguish the quantum numbers of these hidden charm states.

Although the effective Lagrangian method is a convenient tool to catch the qualitative features of the $\gamma p \rightarrow \bar{D}^{*0} \Lambda_c^+$ reaction, the free parameters in the model give it some uncontrollable uncertainties. In the present work, based on phenomenological Lagrangians, we only consider the selected tree-diagram contributions. However, our calculation offers some important clues for the mechanisms of the $\gamma p \rightarrow \bar{D}^{*0} \Lambda_c^+$ reaction and makes a first effort to study the role of the predicted N_{cc}^* states in the $\gamma p \rightarrow \bar{D}^{*0} \Lambda_c^+$ reaction. It is expected that future experimental measurements could test our model and give more information about the $\gamma p \rightarrow \bar{D}^{*0} \Lambda_c^+$ reaction.

This paper is organized as follows. In Section 2, the formalisms and ingredients for our calculations are listed. The results of total and differential cross sections and discussions are presented in Section 3. Finally, a short summary is given in the last section.

2 Formalisms and ingredients

2.1 Feynman diagrams and interaction Lagrangian densities

We study the $\gamma p \rightarrow \bar{D}^{*0} \Lambda_c^+$ reaction within the effective Lagrangian approach, which has been widely employed to investigate photoproduction processes. The basic tree level Feynman diagrams for $\gamma p \rightarrow \bar{D}^{*0} \Lambda_c^+$ reaction are depicted in Fig. 1, where the contributions from the hidden charm N_{cc}^* states [Fig. 1(a)], the nucleon pole [Fig. 1(b)], the D^0 meson exchange [Fig. 1(c)], the Λ_c^+ exchange [Fig. 1(d)], and the contact term [Fig. 1(e)] are taken into account.

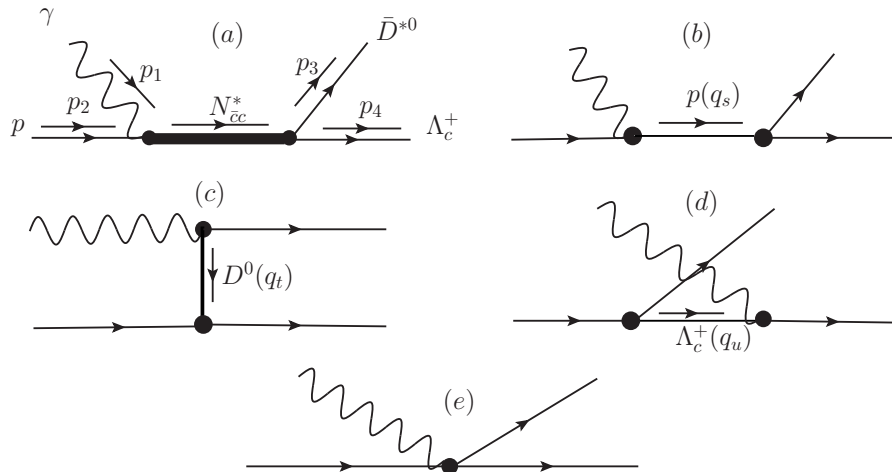


Fig. 1. Feynman diagrams for the $\gamma p \rightarrow \bar{D}^{*0} \Lambda_c^+$ reaction. The contributions from the s -channel N_{cc}^* resonance (a), s -channel nucleon pole (b), t -channel D^0 exchange (c), u -channel Λ_c^+ exchange (d), and contact term (e) are considered. In the first diagram, we also show the definition of the kinematical (p_1, p_2, p_3, p_4) that we use in the present calculation. In addition, we use $q_s = p_1 + p_2$, $q_t = p_1 - p_3$, and $q_u = p_4 - p_1$.

To compute the amplitudes of the diagrams shown in Fig. 1, the effective Lagrangian densities for the relevant interaction vertexes are needed. We adopt the effective Lagrangians as used in Refs. [16–19],

$$\mathcal{L}_{N\gamma N\bar{c}c}^{1/2^-} = \frac{eh}{2M_N}\bar{N}\sigma_{\mu\nu}\partial^\nu A^\mu N_{\bar{c}c}^* + H.c., \quad (1)$$

$$\mathcal{L}_{N\gamma N\bar{c}c}^{3/2^-} = -ie\left[\frac{h_1}{2M_N}\bar{N}\gamma_\nu + \frac{h_2}{(2M_N)^2}\partial_\nu\bar{N}\right]\times F^{\mu\nu}N_{\bar{c}c\mu}^* + H.c., \quad (2)$$

$$\mathcal{L}_{N_{\bar{c}c}^*NJ/\psi}^{1/2^-} = g_{N_{\bar{c}c}^*NJ/\psi}^{1/2^-}\bar{N}\gamma_5\gamma_\mu N_{\bar{c}c}^*\psi^\mu + H.c., \quad (3)$$

$$\mathcal{L}_{N_{\bar{c}c}^*\bar{D}^*\Lambda_c}^{1/2^-} = g_{N_{\bar{c}c}^*\bar{D}^*\Lambda_c}^{1/2^-}\bar{\Lambda}_c\gamma_5\gamma_\mu N_{\bar{c}c}^*\bar{D}^{*0\mu} + H.c., \quad (4)$$

$$\mathcal{L}_{N_{\bar{c}c}^*NJ/\psi}^{3/2^-} = g_{N_{\bar{c}c}^*NJ/\psi}^{3/2^-}\bar{N}N_{\bar{c}c\mu}^*\psi^\mu + H.c., \quad (5)$$

$$\mathcal{L}_{N_{\bar{c}c}^*\bar{D}^*\Lambda_c}^{3/2^-} = g_{N_{\bar{c}c}^*\bar{D}^*\Lambda_c}^{3/2^-}\bar{\Lambda}_c N_{\bar{c}c\mu}^*\bar{D}^{*0\mu} + H.c., \quad (6)$$

$$\mathcal{L}_{\gamma pp} = -e\bar{p}(\gamma^\mu A_\mu - \frac{k_p}{2M_p}\sigma^{\mu\nu}\partial_\nu A_\mu)p, \quad (7)$$

$$\mathcal{L}_{\Lambda_c ND} = ig_{\Lambda_c ND}\bar{\Lambda}_c\gamma_5 ND + H.c., \quad (8)$$

$$\mathcal{L}_{\Lambda_c N\bar{D}^*} = g_{\Lambda_c N\bar{D}^*}\bar{\Lambda}_c\gamma^\mu N\bar{D}_\mu^* + H.c., \quad (9)$$

$$\mathcal{L}_{\gamma\Lambda_c\Lambda_c} = -e\bar{\Lambda}_c(\gamma^\mu A_\mu - \frac{k_{\Lambda_c}}{2M_{\Lambda_c}}\sigma^{\mu\nu}\partial_\nu A_\mu)\Lambda_c, \quad (10)$$

$$\mathcal{L}_{D^*D\gamma} = \frac{e}{4}g_{D^*D\gamma}\epsilon^{\mu\nu\alpha\beta}F_{\mu\nu}\mathcal{D}_{\alpha\beta}^*D + H.c., \quad (11)$$

where $N_{\bar{c}c}^*$ and $N_{\bar{c}c\mu}^*$ are the hidden charm nuclear resonance field with spin-parity $J^P = 1/2^-$ and $J^P = 3/2^-$, respectively. N , A_μ , Λ_c , \bar{D}^* , ψ^μ are the nucleon field, photon field, Λ_c field, D^* field, and J/ψ field, respectively. M_N and M_{Λ_c} are the masses of the nucleon and $\Lambda_c^+(2286)$, while $\epsilon^{\mu\nu\alpha\beta}$ is the Levi-Civita tensor with $\epsilon^{0123} = 1$. In the above Lagrangian densities, the definitions of $\sigma_{\mu\nu}$, $F_{\mu\nu}$, and $\mathcal{D}_{\alpha\beta}^*$ are:

$$\sigma_{\mu\nu} = \frac{i}{2}(\gamma_\mu\gamma_\nu - \gamma_\nu\gamma_\mu), \quad (12)$$

$$F_{\mu\nu} = \partial_\mu A_\nu - \partial_\nu A_\mu, \quad (13)$$

$$\mathcal{D}_{\alpha\beta}^* = \partial_\alpha D_\beta^* - \partial_\beta D_\alpha^*. \quad (14)$$

2.2 Coupling constants and form factors

First, we take the anomalous magnetic momentum $k_p = 1.79$ and $k_{\Lambda_c} = 0.35$ as used in Refs. [20, 21]. The

$$eh = g_{N_{\bar{c}c}^*NJ/\psi}^{1/2^-}\frac{e}{f_{J/\psi}}\frac{2M_N}{(M_{N_{\bar{c}c}^*}^2 - M_N^2)M_{J/\psi}}\sqrt{M_{J/\psi}^2(M_N^2 + 4M_N M_{N_{\bar{c}c}^*} + M_{N_{\bar{c}c}^*}^2) + (M_{N_{\bar{c}c}^*}^2 - M_N^2)^2}, \quad (17)$$

$$eh_1 = g_{N_{\bar{c}c}^*NJ/\psi}^{3/2^-}\frac{e}{f_{J/\psi}}\frac{2M_N(M_N + M_{N_{\bar{c}c}^*})}{(M_{N_{\bar{c}c}^*}^2 - M_N^2)M_{J/\psi}}\sqrt{\frac{6M_{J/\psi}^2 M_{N_{\bar{c}c}^*}^2 + M_N^4 - 2M_N^2 M_{N_{\bar{c}c}^*}^2 + M_{N_{\bar{c}c}^*}^4}{3M_{N_{\bar{c}c}^*}^2 + M_N^2}}. \quad (18)$$

coupling constants for the $\Lambda_c p D$ and $\Lambda_c p D^*$ vertexes are taken to be $g_{\Lambda_c p D} = -13.98$ and $g_{\Lambda_c p D^*} = -5.20$ as obtained in Refs. [18, 19, 22] from $SU(4)$ flavor symmetry.

Second, the coupling constant $g_{D^*D\gamma}$ is determined by the radiative decay width of $D^{*0} \rightarrow D^0\gamma$,

$$\Gamma_{D^{*0} \rightarrow D^0\gamma} = \frac{e^2 g_{D^*D\gamma}^2}{96\pi} M_{D^{*0}}^3 \left(1 - \frac{M_{D^0}^2}{M_{D^{*0}}^2}\right)^3. \quad (15)$$

Unfortunately, information about the decay width $\Gamma_{D^{*0} \rightarrow D^0\gamma}$ is scarce [23]. Thus, it is necessary to rely on theoretical predictions, such as those of Ref. [24], where $\Gamma_{D^{*0} \rightarrow D^0\gamma} = 26$ keV was deduced from the data on strong and radiative decays of D^* mesons. From Eq. (15) we can easily obtain $g_{D^*D\gamma} = 2.0$ GeV $^{-1}$ with $M_{D^{*0}} = 2.007$ GeV, $M_{D^0} = 1.865$ GeV and $\Gamma_{D^{*0} \rightarrow D^0\gamma} = 26$ keV.

Next, we comment on the coupling constants h , h_1 and h_2 for $N_{\bar{c}c}^* N\gamma$ vertexes, where their values will be obtained from the strong coupling constants $g_{N_{\bar{c}c}^*NJ/\psi}^{1/2^-}$ and $g_{N_{\bar{c}c}^*NJ/\psi}^{3/2^-}$ using the vector meson dominance (VMD) model. We adopt the VMD leading order coupling between J/ψ and photon:

$$\mathcal{L}_{J/\psi\gamma} = -\frac{eM_{J/\psi}^2}{f_{J/\psi}}\psi_\mu A^\mu, \quad (16)$$

where $M_{J/\psi}$ and $f_{J/\psi}$ denote the mass and the decay constant of the vector meson J/ψ . With the decay width $\Gamma_{J/\psi \rightarrow e^+e^-} = 5.55$ keV [23], one obtains the parameter $e/f_{J/\psi} = 0.027$.

For the $N_{\bar{c}c}^*$ with $J^P = 3/2^-$, there are two different coupling structures for the $N_{\bar{c}c}^* N\gamma$ vertex, and information about the $N_{\bar{c}c}^* \rightarrow N\gamma$ transition is unknown. Thus, it is necessary to rely on previous theoretical works. As argued in Ref. [11], for $N_{\bar{c}c}^*$ decays into $J/\psi p$, the momentum of the final states are fairly small compared with the nucleon mass. Thus, the higher partial wave terms proportional to $(p/M_N)^2$ can be neglected. Nevertheless, in this work, we will only consider the leading order s -wave $N_{\bar{c}c}^* N\gamma$ coupling and leave the higher partial waves to further studies. Then, we can relate h_1 to the $g_{N_{\bar{c}c}^*NJ/\psi}^{3/2^-}$ for $N_{\bar{c}c}^*$ with $J = 3/2^-$. In the framework of the VMD, the coupling constants h and h_1 are related to the strong coupling constant $g_{N_{\bar{c}c}^*NJ/\psi}^{1/2^-}$ and $g_{N_{\bar{c}c}^*NJ/\psi}^{3/2^-}$ as,

With the $N_{c\bar{c}}^*$ masses and the values of $g_{N_{c\bar{c}}^*NJ/\psi}^{1/2^-}$ that were obtained in Ref. [6], we can easily get the values of eh and eh_1 as shown in Table 1, where we show also

the coupling constants $g_{N_{c\bar{c}}^*\bar{D}^*\Lambda_c}$ that we need to calculate the contributions of the hidden charm $N_{c\bar{c}}^*$ states in the $\gamma p \rightarrow \bar{D}^{*0}\Lambda_c^+$ reaction.

Table 1. Values of the hidden charm $N_{c\bar{c}}^*$ parameters required for the estimation of the $\gamma p \rightarrow \bar{D}^{*0}\Lambda_c^+$ reaction. Their masses, widths and strong coupling were predicted in Ref. [6]. The coupling eh is for $N_{c\bar{c}}^*$ with $J^P = 1/2^-$, while eh_1 is for $N_{c\bar{c}}^*$ with $J^P = 3/2^-$.

$N_{c\bar{c}}^*$	J^P	Mass (MeV)	Width (MeV)	$g_{N_{c\bar{c}}^*\bar{D}^*\Lambda_c}$	$g_{N_{c\bar{c}}^*NJ/\psi}$	eh (or eh_1)
N_1^*	$\frac{1}{2}^-$	4262	35.7	0.50	0.76	0.018
N_2^*	$\frac{1}{2}^-$	4410	58.9	0.20	1.44	0.034
N_3^*	$\frac{1}{2}^-$	4481	57.8	0.12	0.72	0.017
N_4^*	$\frac{3}{2}^-$	4334	38.8	0.28	1.32	0.031
N_5^*	$\frac{3}{2}^-$	4417	8.22	0.11	0.53	0.012
N_6^*	$\frac{3}{2}^-$	4481	35.8	0.20	1.05	0.024

In evaluating the scattering amplitudes of the $\gamma p \rightarrow \bar{D}^{*0}\Lambda_c^+$ reaction, we need to include the form factors because hadrons are not pointlike particles. For the t -channel D^0 meson exchange, we adopt here a common scheme used in many previous works [22, 25, 26],

$$\mathcal{F}_{D^0}(q_t^2) = \left(\frac{\Lambda_{D^0}^2 - M_{D^0}^2}{\Lambda_{D^0}^2 - q_t^2} \right)^2, \quad (19)$$

with cutoff parameter $\Lambda_{D^0} = 2.5$ GeV.

For the s -channel and u -channel processes, we adopt a form factor [25, 26]

$$\mathcal{F}_B(q_{ex}^2, M_{ex}) = \frac{\Lambda_B^4}{\Lambda_B^4 + (q_{ex}^2 - M_{ex}^2)^2}, \quad (20)$$

where q_{ex} and M_{ex} are the four-momentum and the mass of the exchanged hadron, respectively. For simplicity, we take $\Lambda_B = 0.5$ GeV [26] for the s -channel nucleon pole, the u -channel Λ_c^+ processes and the s -channel resonance exchanges. The numerical results are not sensitive to the value of Λ_B because of the narrow width of the hidden charm resonances, but the results of the t -channel D^0 exchange are sensitive to the value of the cutoff parameter Λ_{D^0} . We will come to this point below.

The propagator for the exchanged D^0 meson used in our calculation is

$$G_{D^0}(q_t) = \frac{i}{q_t^2 - M_{D^0}^2}. \quad (21)$$

For the propagator of the spin-1/2 and 3/2 baryon, we take

$$G_{1/2}(q) = \frac{i(q + M)}{q^2 - M^2 + iM\Gamma}, \quad (22)$$

$$G_{3/2}^{\mu\nu}(q) = \frac{i(q + M)P^{\mu\nu}(q)}{q^2 - M^2 + iM\Gamma}, \quad (23)$$

with

$$P^{\mu\nu} = -g^{\mu\nu} + \frac{1}{3}\gamma^\mu\gamma^\nu + \frac{1}{3M}(\gamma^\mu q^\nu - \gamma^\nu q^\mu) + \frac{2}{3M^2}q^\mu q^\nu, \quad (24)$$

where q and M stand for the four-momentum and the mass of the intermediate nucleon pole, Λ_c^+ state and $N_{c\bar{c}}^*$ resonance that are shown in Table 1, respectively. Since $q^2 < 0$ for u -channel Λ_c^+ exchange, we take $\Gamma = 0$ for Λ_c^+ and also for the nucleon pole, while for the hidden charm $N_{c\bar{c}}^*$ resonance, we take their widths as shown in Table 1.

2.3 Scattering amplitudes

With the above effective Lagrangian densities, the scattering amplitudes for the $\gamma p \rightarrow \bar{D}^{*0}\Lambda_c^+$ reaction can be obtained straightforwardly. First, we write the scattering amplitudes for the $N_{c\bar{c}}^*$ resonance with $J^P = 1/2^-$ and $3/2^-$

$$\begin{aligned} \mathcal{M}_a^{1/2} &= ig_{N_{c\bar{c}}^*\bar{D}^{*0}\Lambda_c}^{1/2^-} \bar{u}_{\Lambda_c}(p_4, s_4) \gamma_5 \gamma_\mu \frac{(q_s + M_{N^*})}{s - M_{N^*}^2 + iM_{N^*}\Gamma} \\ &\times \mathcal{F}_{N^*}(s, M_{N^*}) \frac{eh_1}{4M_N} \gamma_5 (\gamma_\nu \not{p}'_1 - \not{p}'_1 \gamma_\nu) \\ &\times u(p_2, s_2) \epsilon^\nu(p_1, s_1) \epsilon^{*\mu}(p_3, s_3), \end{aligned} \quad (25)$$

$$\begin{aligned} \mathcal{M}_a^{3/2} &= -ig_{N_{c\bar{c}}^*\bar{D}^{*0}\Lambda_c}^{3/2^-} \bar{u}_{\Lambda_c}(p_4, s_4) \frac{(q_s + M_{N^*})P^{\mu\eta}}{s - M_{N^*}^2 + iM_{N^*}\Gamma} \\ &\times \mathcal{F}_{N^*}(s, M_{N^*}) \frac{eh_1}{2M_N} [p_{1\eta} \gamma_\nu - \not{p}'_1 g_{\eta\nu}] \\ &\times u(p_2, s_2) \epsilon^{*\mu}(p_3, s_3) \epsilon_\nu(p_1, s_1), \end{aligned} \quad (26)$$

for Fig. 1(a), and

$$\begin{aligned} \mathcal{M}_b &= -ie g_{\Lambda_c p \bar{D}^0} \frac{1}{s - M_N^2} \mathcal{F}_N(s, M_N) \epsilon^\nu(p_1, s_1) \\ &\times \epsilon^{*\mu}(p_3, s_3) \bar{u}_{\Lambda_c}(p_4, s_4) \gamma_\mu (\not{q} + M_N) \\ &\times \left[\gamma_\nu - \frac{k_p}{4M_N} (\gamma_\nu \not{p}_1 - \not{p}_1 \gamma_\nu) \right] u(p_2, s_2), \end{aligned} \quad (27)$$

$$\begin{aligned} \mathcal{M}_c &= -\frac{e}{4} g_{\bar{D}^0} g_{D^0} g_{\Lambda_c p D^0} \frac{1}{t - M_{D^0}^2} \mathcal{F}_M^2(t) \\ &\times \epsilon^\nu(p_1, s_1) \epsilon^{*\mu}(p_3, s_3) \epsilon^{\eta\sigma\alpha\beta} [p_{1\eta} g_{\sigma\nu} - p_{1\sigma} g_{\eta\nu}] \\ &\times [p_{3\alpha} g_{\mu\beta} - p_{3\beta} g_{\alpha\mu}] \bar{u}_{\Lambda_c}(p_4, s_4) \gamma_5 u(p_2, s_2), \end{aligned} \quad (28)$$

$$\begin{aligned} \mathcal{M}_d &= -ie g_{\Lambda_c p \bar{D}^*} \frac{1}{u - M_{\Lambda_c}^2} \mathcal{F}_{\Lambda_c}(u, M_{\Lambda_c}) \epsilon^\nu(p_1, s_1) \\ &\times \epsilon^{*\mu}(p_3, s_3) \bar{u}_{\Lambda_c}(p_4, s_4) \left[\gamma_\nu - \frac{k_{\Lambda_c}}{4M_{\Lambda_c}} (\gamma_\nu \not{p}_1 - \not{p}_1 \gamma_\nu) \right] \\ &\times (\not{q}_u + M_{\Lambda_c}) \gamma_\mu u(p_2, s_2), \end{aligned} \quad (29)$$

for Figs. 1(b), 1(c), and 1(d), respectively. In the above equations, $s = q_s^2$, $t = q_t^2$, and $u = q_u^2$ indicate the Mandelstam variables.

The contact term illustrated in Fig. 1(e) serves to keep the full amplitude gauge invariant. For the present calculation, we adopt the following form [16, 27],

$$\begin{aligned} \mathcal{M}_e &= ie g_{\Lambda_c p \bar{D}^*} \bar{u}_{\Lambda_c}(p_4, s_4) \gamma^\mu C^\nu u(p_2, s_2) \\ &\times \epsilon^\nu(p_1, s_1) \epsilon^{*\mu}(p_3, s_3), \end{aligned} \quad (30)$$

where C^ν is expressed as

$$\begin{aligned} C^\nu &= (2p_2 - p_1)^\nu \frac{\mathcal{F}_N(s, M_N) - 1}{s - m_N^2} \mathcal{F}_{\Lambda_c}(u, M_{\Lambda_c}) \\ &+ (2p_4 - p_1)^\nu \frac{\mathcal{F}_{\Lambda_c}(u, M_{\Lambda_c}) - 1}{u - m_{\Lambda_c}^2} \mathcal{F}_N(s, M_N). \end{aligned} \quad (31)$$

The differential cross section in the center of mass (c.m.) frame for the $\gamma p \rightarrow \bar{D}^* \Lambda_c^+$ reaction is calculated using the following equation:

$$\frac{d\sigma}{d\cos\theta} = \frac{M_N M_{\Lambda_c}}{32\pi s} \frac{|\vec{p}_3^{\text{c.m.}}|}{|\vec{p}_1^{\text{c.m.}}|} \sum_{s_1, s_2, s_3, s_4} |\mathcal{M}_{\gamma p \rightarrow \bar{D}^* \Lambda_c^+}|^2, \quad (32)$$

where $\mathcal{M}_{\gamma p \rightarrow \bar{D}^* \Lambda_c^+} = \mathcal{M}_a + \mathcal{M}_b + \mathcal{M}_c + \mathcal{M}_d + \mathcal{M}_e$ is the total scattering amplitude of the $\gamma p \rightarrow \bar{D}^* \Lambda_c^+$ reaction, and θ is the scattering angle of the outgoing \bar{D}^* meson relative to the beam direction, while $\vec{p}_1^{\text{c.m.}}$ and $\vec{p}_3^{\text{c.m.}}$ are the photon and \bar{D}^* three momenta in the c.m. frame, which are

$$|\vec{p}_1^{\text{c.m.}}| = \frac{\lambda^{1/2}(s, 0, M_N^2)}{2\sqrt{s}}, \quad (33)$$

$$|\vec{p}_3^{\text{c.m.}}| = \frac{\lambda^{1/2}(s, M_{\bar{D}^*}^2, M_{\Lambda_c}^2)}{2\sqrt{s}}, \quad (34)$$

where λ is the Källén function with $\lambda(x, y, z) = (x - y - z)^2 - 4yz$.

3 Numerical results

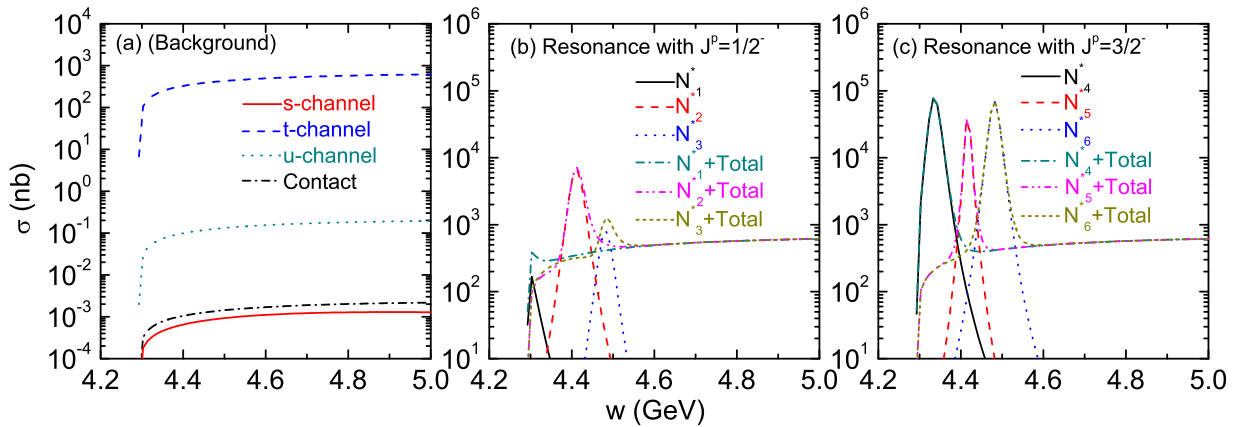


Fig. 2. (Color online) The total cross sections of the $\gamma p \rightarrow \bar{D}^* \Lambda_c^+$ reaction. (a) shows the cross section of the background contributions including the s -channel nucleon pole (red solid), the t -channel D^0 exchange (blue dashed), $\Lambda_c^+(2286)$ as an intermediate state in the u -channel (dark cyan dotted) and the contact term (black dash-dotted). (b) and (c) indicate the contributions of the total and s -channel processes with an N_{cc}^* resonance of $J = 1/2$ and $J = 3/2$, respectively.

In this section, we show our theoretical results for the total and differential cross sections of the $\gamma p \rightarrow \bar{D}^{*0}\Lambda_c^+$ reaction near the threshold. In Fig. 2 we show our numerical results for the total cross section as a function of the invariant mass $W = \sqrt{s}$ of the γp system. We take the contributions from the nucleon pole in the s -channel, Λ_c^+ exchange in the u -channel, D^0 exchange in the t -channel, and the contact term as the background contribution. From Fig. 2 (a), we see that the contribution of D^0 exchange is larger than the other background contributions. From Figs. 2 (b) and (c), one can see that on top of these background contributions the peaks of the hidden charm $N_{c\bar{c}}^*$ resonances are clearly seen. In particular, the contributions from $N_{c\bar{c}}^*$ resonances with $J^P = 3/2^-$ are significant because of their narrow widths.

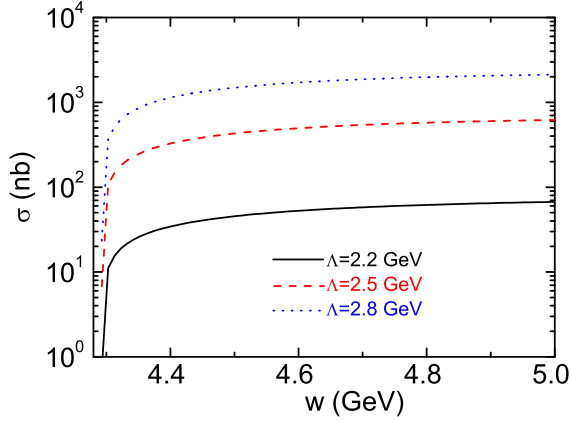


Fig. 3. (Color online) The cross section of the t -channel D^0 exchange for the $\gamma p \rightarrow \bar{D}^{*0}\Lambda_c^+$ reac-

tion with different Λ_{D^0} values.

The contribution of t -channel D^0 exchange is sensitive to the value of the cutoff parameter Λ_{D^0} . To see how much it depends on the cutoff parameter Λ_{D^0} , in Fig. 3 we show the predicted cross sections of the D^0 exchange with three typical cutoff parameters $\Lambda_{D^0} = 2.2, 2.5, 2.8$ GeV, respectively. From the figure, it can be clearly seen that the predicted cross sections have a strong dependence on the cutoff parameter Λ_{D^0} . The total cross section reduces by a factor of 10 when Λ_{D^0} decreases from 2.5 to 2.2 GeV.

In addition to the total cross section, we present in Figs. 4 and 5 the angular distributions of the $\gamma p \rightarrow \bar{D}^{*0}\Lambda_c^+$ reaction at different energies. i.e. $W = 4.3$ GeV, 4.4 GeV, and 4.5 GeV. The results of the $N_{c\bar{c}}$ resonances are shown with the red-dashed curves. The contributions of backgrounds are shown with black-solid curves. From Figs. 4 and 5 one can see that the s -channel hidden charmed $N_{c\bar{c}}^*$ contributions are restricted to a narrow kinematic region because of the narrow widths of these $N_{c\bar{c}}^*$ states. Away from the $N_{c\bar{c}}^*$ resonance region the t -channel D^0 exchange plays a dominant role. The contributions from the $N_{c\bar{c}}^*$ states make the differential cross section flat because these $N_{c\bar{c}}^*$ states decay into $J/\psi p$ in s -wave, which is different from the diffractive behavior of the background contributions as shown by Figs. 4, and 5. It should be pointed out, if any other possible states also couple to $\bar{D}^*\Lambda_c^+$ strongly, they will also cause nondiffractive effects at off-forward angles which can be measured directly. We hope that this feature may be used to study the $N_{c\bar{c}}^*$ resonance in future experiments.

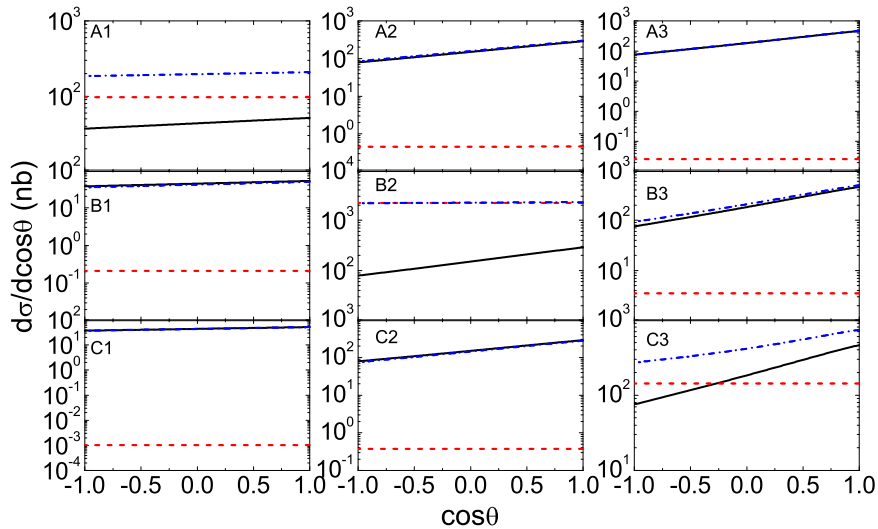


Fig. 4. (Color online) Angular distributions of the $\gamma p \rightarrow \bar{D}^{*0}\Lambda_c^+$ reaction including the contributions of $N_{c\bar{c}}^*$ resonances with $J^P = 1/2^-$ at different energies: $W = 4.3$ GeV (A1, B1, and C1), 4.4 GeV (A2, B2, and C2), and 4.5

GeV ($A3$, $B3$, and $C3$). $A1$, $A2$, and $A3$ are for N_1^* ; $B1$, $B2$, and $B3$ are for N_2^* ; $C1$, $C2$, and $C3$ are for N_3^* .

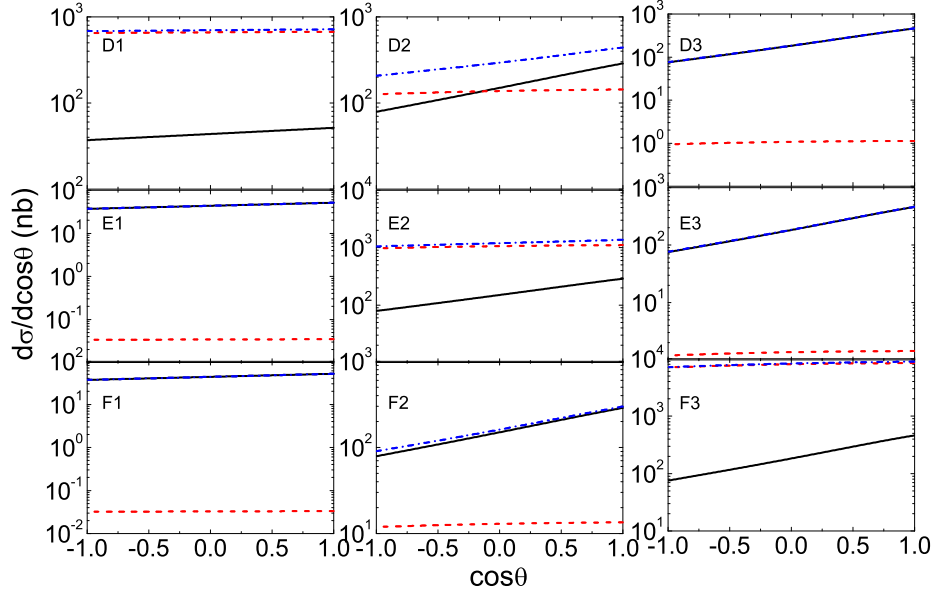


Fig. 5. (Color online) Angular distributions of the $\gamma p \rightarrow \bar{D}^{*0} \Lambda_c^+$ reaction including the contributions of N_{cc}^* resonances with $J^P = 3/2^-$ at different energies: $W = 4.3$ GeV ($D1$, $E1$, and $F1$), 4.4 GeV ($D2$, $E2$, and $F2$), and 4.5 GeV ($D3$, $E3$, and $F3$). $D1$, $D2$, and $D3$ are for N_4^* ; $E1$, $E2$, and $E3$ are for N_5^* ; $F1$, $F2$, and $F3$ are for N_6^* .

4 Summary

We have studied the total and differential cross sections of the $\gamma p \rightarrow \bar{D}^{*0} \Lambda_c^+$ reaction within the effective Lagrangian model. In addition to the background contributions from the s -channel nucleon pole, t -channel D^0 exchange, $\Lambda_c^+(2286)$ as an intermediate state in the u -channel and the contact term, we checked also the contributions from the s -channel hidden charm N_{cc}^* resonances which were dynamically generated from the interaction between charmed mesons and charmed baryons as reported in Refs. [4–6]. The results of the total cross section show clear peak structures due to the excitations of the hidden-charm N_{cc}^* states. We also evaluated the differential cross sections for different energies and found that the contributions of the N_{cc}^* resonances in the s -channel are much different from the background contributions. A detailed scan of the total and differential cross section in the low energy region of the $\gamma p \rightarrow \bar{D}^{*0} \Lambda_c^+$ reaction will help us to study the hidden charm N_{cc}^* states.

Furthermore, the two observed P_c states were investigated in Refs. [28–30] and it was shown that the $J/\psi p$

invariant mass spectrum in the $\Lambda_b \rightarrow J/\psi K^- p$ decay can be reproduced by triangle rescattering due to the reaction dynamics and the peculiar kinematics. The mechanism is called the triangle singularity, and may produce threshold enhancements to mimic the behavior of genuine states or to contribute on top of the genuine states. If these hidden charm states are genuine states, they should be created in the $\gamma p \rightarrow \bar{D}^{*0} \Lambda_c^+$ reaction, while if they are the triangle singularity enhancement, they will not appear in the $\gamma p \rightarrow \bar{D}^{*0} \Lambda_c^+$ reaction because the triangle singularity condition cannot be satisfied here. Therefore, study of the $\gamma p \rightarrow \bar{D}^{*0} \Lambda_c^+$ reaction could help us to understand the nature of these hidden charm states and also the two pentaquark P_c states that were observed by LHCb collaboration [1].

Finally, we would like to stress that, thanks to the important role played by the s -channel resonant contribution in the $\gamma p \rightarrow \bar{D}^{*0} \Lambda_c^+$ reaction, future experimental data for this reaction can be used to improve our knowledge of hidden charm N_{cc}^* properties, which are at present poorly known. This work constitutes a first step in this direction.

References

- 1 R. Aaij *et al.* [LHCb Collaboration], Phys. Rev. Lett. **115**, 072001 (2015)
- 2 H. X. Chen, W. Chen, X. Liu and S. L. Zhu, Phys. Rept. **639**, 1 (2016)
- 3 Z. C. Yang, Z. F. Sun, J. He, X. Liu and S. L. Zhu, Chin. Phys. C **36**, 6 (2012)
- 4 J. J. Wu, R. Molina, E. Oset and B. S. Zou, Phys. Rev. Lett. **105**, 232001 (2010)
- 5 J. J. Wu, R. Molina, E. Oset and B. S. Zou, Phys. Rev. C **84**, 015202 (2011)
- 6 C. W. Xiao, J. Nieves and E. Oset, Phys. Rev. D **88**, 056012 (2013)
- 7 L. Roca, J. Nieves and E. Oset, Phys. Rev. D **92**, 094003 (2015)
- 8 L. Roca and E. Oset, arXiv:1602.06791 [hep-ph].
- 9 C. W. Shen, F. K. Guo, J. J. Xie and B. S. Zou, "Disentangle the hadronic molecule nature of the $P_c(4380)$ pentaquark-like structure," arXiv:1603.04672 [hep-ph].
- 10 Y. Huang, J. He, H. F. Zhang and X. R. Chen, J. Phys. G **41** (2014) 11, 115004
- 11 Q. Wang, X. H. Liu and Q. Zhao, Phys. Rev. D **92**, 034022 (2015)
- 12 V. Kubarovsky and M. B. Voloshin, Phys. Rev. D **92**, 031502 (2015)
- 13 X. Y. Wang and X. R. Chen, Eur. Phys. J. A **51**, 85 (2015)
- 14 Q. F. Li, X. Y. Wang, J. J. Xie, X. R. Chen and Y. B. Dong, Phys. Rev. D **93**, 034009 (2016)
- 15 E. J. Garzon and J. J. Xie, Phys. Rev. C **92**, 035201 (2015)
- 16 Y. Oh, C. M. Ko and K. Nakayama, Phys. Rev. C **77**, 045204 (2008)
- 17 B. S. Zou and F. Hussain, Phys. Rev. C **67**, 015204 (2003)
- 18 Y. Dong, A. Faessler, T. Gutsche and V. E. Lyubovitskij, Phys. Rev. D **90**, 094001 (2014)
- 19 Y. Dong, A. Faessler, T. Gutsche, S. Kumano and V. E. Lyubovitskij, Phys. Rev. D **82**, 034035 (2010)
- 20 S. N. Jena and D. P. Rath, Phys. Rev. D **34**, 196 (1986).
- 21 J. J. Xie and J. Nieves, Phys. Rev. C **82**, 045205 (2010)
- 22 J. J. Xie, Y. B. Dong and X. Cao, Phys. Rev. D **92**, 034029 (2015)
- 23 K. A. Olive *et al.* [Particle Data Group Collaboration], Chin. Phys. C **38**, 090001 (2014).
- 24 Y. b. Dong, A. Faessler, T. Gutsche and V. E. Lyubovitskij, Phys. Rev. D **77**, 094013 (2008)
- 25 P. Gao, J. J. Wu and B. S. Zou, Phys. Rev. C **81**, 055203 (2010)
- 26 S. H. Kim, S. i. Nam, Y. Oh and H. C. Kim, Phys. Rev. D **84**, 114023 (2011)
- 27 H. Haberzettl, Phys. Rev. C **56**, 2041 (1997)
- 28 F. K. Guo, U. G. Meißer, W. Wang and Z. Yang, Phys. Rev. D **92**, 071502 (2015)
- 29 X. H. Liu, Q. Wang and Q. Zhao, Phys. Lett. B **757**, 231 (2016)
- 30 M. Mikhasenko, arXiv:1507.06552 [hep-ph].